JJMIE

Jordan Journal of Mechanical and Industrial Engineering

Volume 14, Number 1, March. 2020
ISSN 1995-6665
Pages 149 - 158

Acceleration Sensor Abnormality Detection Method for Axle Box of Unmanned Vehicle

Jianhu Gong

School of Data and Computer Science, Guangdong Peizheng College, Guangzhou 510830, China

Received OCT 16 2019 *Accepted JAN 20 2020*

Abstract

The method of detecting the acceleration sensor anomaly of the axle box of unmanned vehicle is studied in this paper. The condition monitoring device needs to install the acceleration sensor on the bogie, which collects the acceleration sensor signal of the axle box of the vehicle. According to each frequency, the vertical vibration acceleration of the axle box with the vertical vibration acceleration of the bogie frame are compared to detect the shock absorber anomaly of axle box; the quasi-double-layer chloroprene rubber filter is used to isolate the high frequency component of shock acceleration signal, while the low frequency component is retained. The vertical displacement of the axle box is obtained by integrating the vertical vibration acceleration of the collected axle box twice. The displacement is the rail corrugation. The sliding variance window statistical algorithm of axle box acceleration is used to obtain the sliding variance of axle box acceleration, and find out the line problems and their corresponding positions. The results show that when the vibration frequency of axle box vibrator is higher than 7.5 Hz, the amplitude ratio of axle box acceleration under the condition of throttle hole blockage and insufficient hydraulic oil is inconsistent with that under the intact condition. At this time, the shock absorber of axle box is abnormal. When the frequency is higher than 8 Hz, the acceleration response ratio of axle box under the three conditions moves towards the same direction, but there are obvious differences. At this time, the shock absorber of axle box attenuates and has abnormal vibration. Based on the analysis of sliding variance of vertical acceleration of axle box before and after rail pre-grinding at 300 km/h speed level, it is concluded that the variance of axle box acceleration decreases, and the effect of rail pre-grinding on improving the smoothness of rail welded joints is very obvious. When the vehicle derails, the vertical vibration acceleration waveform of axle box and the vibration acceleration waveform of bogie on ballast track show that the absolute value of negative peak vibration acceleration is greater than that of positive peak vibration acceleration.

Keywords: Unmanned vehicle; Sensor; Axle box; Acceleration; Abnormal detection; Inertia principle;

1. Introduction

In recent years, with the increasing demand for active safety and intelligence of automobiles in the market, the huge social and economic value of unmanned driving has become increasingly prominent. More and more enterprises and scientific research institutions actively participate in and promote the development of the field of unmanned driving [1]. At present, there is no formal mass production and sales of completely unmanned vehicles, but a considerable number of experimental vehicles can achieve highly autonomous driving behavior through environmental awareness, such as starting, acceleration, braking, lane tracking, lane change, collision avoidance, and parking, etc. [2]. For the definition of unmanned driving, it divides unmanned driving into five levels, namely advanced auxiliary driving, specific function assistance, combined function assistance, highly automatic driving, and completely unmanned driving. At present, most of the vehicles are still at the stage of combined function assistance. There is still a long way to go to accomplish the production of completely unmanned vehicles.

Vibration sensors are also called vibration detectors. They are similar to seismographs that record seismic and atomic bomb explosion waves. They are the most common ones used in sensors. This kind of sensor detects the target mainly by capturing the ground vibration signal caused by the movement of human or maneuvering target through the vibration probe (also called seismograph) of the device [3]. Vibration sensor has a long detection distance and high sensitivity. At the same time, the vibration sensor also has a certain target resolution[4]. It can distinguish not only man-made vibration and natural disturbance, but also people and targets. Usually, vibration sensor is used to collect abnormal acceleration signals of vehicles[5].

Foreign scholars have done a lot of research on the detection of acceleration sensor anomaly of axle box of unmanned vehicle in this field: Morys established a vehicle-track coupling model, believing that wheel non-circularization would cause a great change in vertical force of wheel and rail, stimulate bending vibration of axle pair, and then lead to lateral sliding of wheel and lateral stripping of material between wheel and rail surface. However, this model did not compare the difference between the amplitude-frequency domain and the frequency domain. Johansson et al. established a three-dimensional numerical model of vehicle-track dynamic interaction and wheel wear feedback coupling. By analyzing the frequency spectrum of wheel-rail force at 50km/h running speed, it was found that

* Corresponding author e-mail: gscilw@163.com.

the larger peak value at 40 Hz came from the vertical resonance of wheel-rail coupling system, corresponding to the fifth, sixth and seventh order polygon wear of wheel, but it did not consider using the statistical analysis method of axle box acceleration sliding variance window to achieve a comprehensive evaluation of track status (sliding variance peak method); CLAUS et al. believed that when the speed exceeds 200 km/h, the third and fourth order polygon wear of wheels could cause significant vibration of the vehicle body at 70 Hz to 100 Hz. Although the purpose of axle box detection was achieved, the repeated impact of trains passing track joints was not considered. Bad sensors or zero drift would lead to the distortion of test signals. Therefore, the method of detecting the acceleration sensor anomaly of axle box of unmanned vehicle studied in this paper provides an effective basis for ensuring the safe operation of unmanned vehicle.

2. Definition of Algorithm

2.1. System Structure of Monitoring Device and Abnormal Detection of Shock Absorber of Axle Box

2.1.1. Structure of Condition Monitoring Device

Figure 1 is the basic structure of the condition monitoring device.

The device assumes that acceleration sensors are installed on bogies, and in order to improve the accuracy of diagnosis and increase monitoring items [6], the way of installing axle box acceleration sensors on specific axles is also studied.

2.1.2. Structure of Monitoring System

The system structure is shown in Figure 2.

Figure 2 shows that the accelerometer measures the vibration acceleration of the axle box of a vehicle, the analog processing is carried out by signal amplifier to quantify the data acquisition card, and the speed sensor collects the train speed [7]. Then the acceleration signal of the axle box is processed by digital processing technology, including noise reduction, digital integration and high-pass filtering. Finally, the waveform of corrugation is obtained.

2.1.3. Abnormal Detection of Shock Absorber of Axle Box

The following will introduce the application of numerical simulation technology to research and test the shock absorber of axle box if there is a fault, which will have an impact on the operation safety. Therefore, a numerical simulation model of single vehicle with 17 degrees of freedom is established. The model assumes that the body shown in Figure 3 is a rigid body with a running speed of 275 km/h. According to the input parameters [8,9], the “white” noise concerned in vehicle vibration modes is listed as a band-limited waveform when the frequency reaches 80 Hz, which is used as track irregularity.

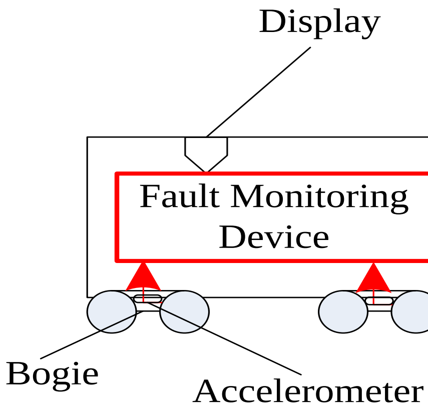

Figure 1. Basic Structure of Condition Monitoring Device

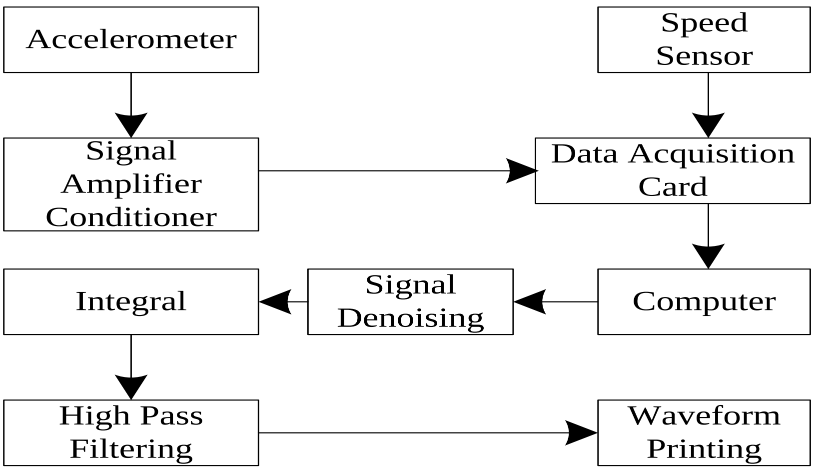

Figure 2. Structure Diagram of Monitoring System

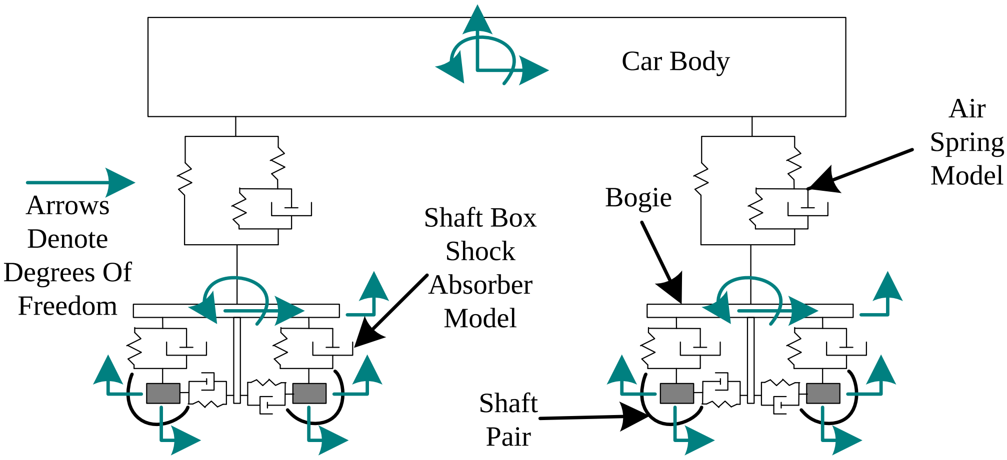

Figure 3. A Numerical Simulation Model for the Vertical System of a Bicycle

The detection method is to compare the vertical vibration acceleration of the newly built or maintained bogie with that of the running bogie according to each frequency. In addition, for vehicles with vertical vibration acceleration sensor of axle box installed for bearing detection, the vertical vibration acceleration of axle box can also be detected by comparing the vertical vibration acceleration of axle box with the vertical vibration acceleration of bogie frame according to each frequency. The former has the advantage that it is not necessary to install vertical acceleration sensor on axle box, but it is necessary to compare track irregularities to the same extent. Because the ratio of vertical vibration acceleration of axle box to the vertical vibration acceleration of bogie frame is used [10], the latter has the advantage of not being affected by track irregularity.

2.2. Impulse Isolation Filter and Detection Principle

2.2.1. Structure and Characteristic Analysis of Impulse Isolation Filter

In order to simulate and reproduce the vibration state of the train running on the rolling vibration test bench, it is necessary to measure the vibration acceleration signal of the train's axle box on the spot. In order to reproduce the vibration of a train running on a straight track, it is necessary to isolate the shock wave when the train passes through the rail seam [11]; the shock acceleration value of the train passing through the rail seam is more than 400 g, while the vibration acceleration of the train running on a straight track is usually less than 10 g. In order to ensure the test accuracy, a sensor with a measuring range of about 15 g should be selected. In addition, in the process of on-line measurement, the repeated impact of rail joint will damage the sensor or cause zero drift, which will lead to the distortion of the test signal. Therefore, in the process of measuring vehicle's axle box acceleration signal, isolation filtering of impact acceleration becomes an urgent research topic. In order to ensure the validity of the measured signal, it is required that the amplitude-frequency characteristics of the impulse isolation filter have good linear smoothness in the low frequency band, and that it should have as steep attenuation characteristics as possible in the high frequency band; at the same time, the cut-off frequency of the filter should be low; when the high frequency components of the impulse acceleration signal are isolated, the low frequency components can be easily processed [12]. According to these requirements, a quasi-double-layer chloroprene rubber filter with good filtering characteristics is designed after repeated analysis and experimental comparison of various shock isolation filters.

The typical spectrum lines of train's axle box vibration and shock are shown in Figure 4 and Figure 5 shows the ideal amplitude-frequency characteristics.

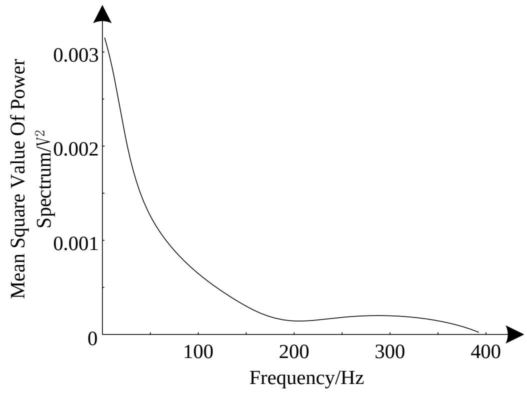

Figure 4. Vibration and Shock Power Spectrum Axle Box

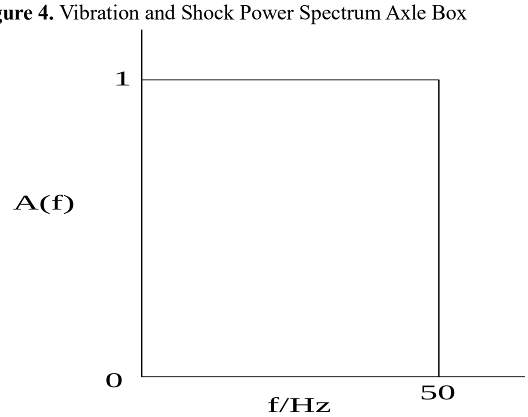

Figure 5. Characteristics of Ideal Impulse of Isolation Filter

As can be seen from Figure 4, the frequency range of shock spectrum is generally below 300 Hz. Considering that the frequency range of vibration acceleration signal of train's axle box due to track irregularity is generally below 50 Hz. It is required that the amplitude-frequency characteristics of the shock isolation filter designed be linear at least before 50 Hz.

The structure of the shock isolation filter is shown in Figure 6. The upper and lower layers of the filter are tightly bonded with the middle layer through 502 glue. The middle layer is 8 mm thick and has a small crack in the chloroprene rubber isolation layer. It can also be called quasi-double rubber filter. The dynamic characteristics of single-layer rubber filter can be described by the physical model shown in Figure 7. Its mathematical equation of motion is as follows:

$$m\ddot{x}+c\dot{x}+kx=P_0 cos\omega t \quad (1)$$

The transfer rate of acceleration can be calculated from the formula.

$$A=\frac{\sqrt{1+\left(2\frac{c}{C_c}\cdot\frac{\omega}{\omega_m}\right)^2}}{\sqrt{\left(1-\frac{\omega}{\omega_m^2}\right)^2+\left(2\frac{c}{C_c}\cdot\frac{\omega}{\omega_m}\right)^2}} \quad (2)$$

In formula (2), $\omega_m=\sqrt{k/m}$ is the natural frequency and $C_c=2\sqrt{mk}$ is the critical damping coefficient. For chloroprene rubber, the elastic coefficient k is independent of frequency, and the product of damping coefficient C and vibration frequency is constant. The formula (2) can be simplified as follows:

$$A=\frac{\sqrt{1+l^2}}{\sqrt{\left(1-\frac{\omega^2}{\omega_m^2}\right)^2+l^2}} \quad (3)$$

In formula (3), $l=(\omega c)/k$ is a constant, and the acceleration transfer rate A here is the amplitude-frequency characteristic $A(f)$ of the filter. The curve is shown in Figure 8. From the curve of Figure 8, it can be seen that the amplitude-frequency characteristics of single rubber layer cannot meet the requirements of impulse signal filtering that the transmission rate at resonance is small, and the transmission rate curve should drop steeply after crossing the resonance region. Considering the above-mentioned single-layer isolation filter system according to these requirements shows many shortcomings. In this paper, a quasi-double rubber filter is designed on the basis of a large number of analysis and experiments [13]. The filter can effectively meet the requirements of shock isolation filter.

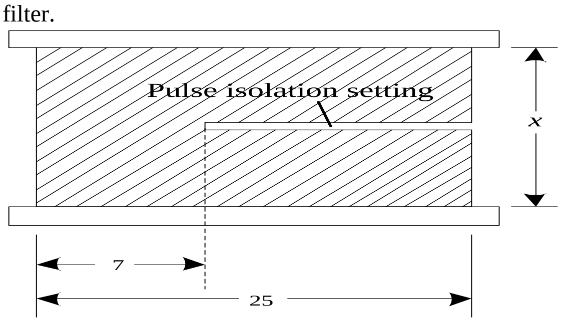

Figure 6. Structural Sketch of Impulse Isolation Filter

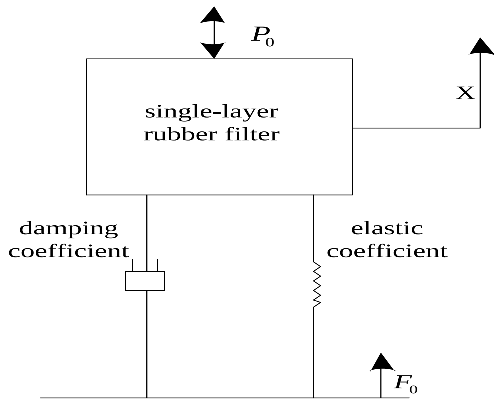

Figure 7. Physical Model of Dynamic Responseof Single Layer Rubber

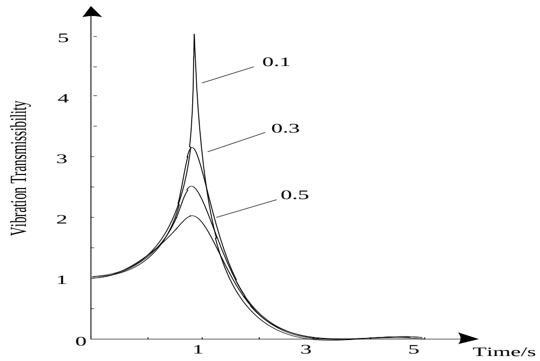

Figure 8. Acceleration Transfer Rate of Monolayer Rubber

2.2.2. Detection Principle

At present, there are two main detection methods for track irregularity: chord measurement method and inertial reference method. The transfer function of the chord measurement method is not always equal to 1, which cannot correctly reflect the real track irregularity [14]. In this paper, the inertia reference method is adopted. The traditional principle of inertia reference method is to install acceleration sensors on the train body. When the vibration frequency of axle box is very high and far higher than the natural frequency of mass spring system composed of vehicle body and wheel axle box, according to the principle of inertia, the vehicle body cannot move up and down along with the axle box, so the vehicle body becomes a static reference which can be used for measurement. Therefore, the displacement of axle box relative to vehicle body is track irregularity without the wheel leaving the rail. However, the vibration frequencies of the axle box caused by rail corrugation are not all much higher than the natural frequencies of the system [15]. When the wavelength is longer or the driving speed is lower, the axial vibration frequencies caused by rail corrugation are not high enough, and the vehicle body will move with it, and the measurement datum will be lost. For this reason, another kind of axle box acceleration integration method based on inertia principle that seems to be more convenient and feasible is proposed, that is, the second integration of the collected vertical vibration acceleration of axle box, indicating that the vertical displacement of the axle box is equal to the rail corrugation, and its detection schematic diagram is shown in Figure 9.

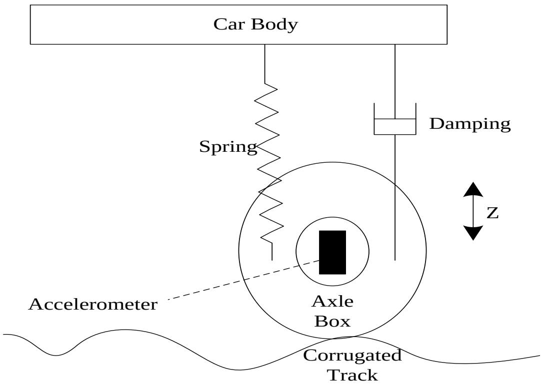

Figure 9. Principle Diagram of Inertial Constant Method

The acceleration vibration signal collected by the acceleration sensor installed on the axle box directly reflects the irregular state of the track. The vertical displacement Z obtained by integration is the wave wear value.

$$Z = \iint \ddot{Z} dt dt \tag{4}$$

At this time, the inertial reference line is the axle box, so the integral value Z is the track wave wear value.

2.3 Statistical Algorithm of Sliding Variance Window for Axle Box Acceleration and Selection of Sliding Window Width

2.3.1 Statistical Algorithm of Sliding Variance Window for Axle Box Acceleration

Variance is the average of the square of the difference between each data and the average. For a group of data $X_n = \{x_1, x_2, x_3, ..., x_n\}$, the definition of variance $D(X_n)$ is shown in formula (5):

$$D(X_n) = \frac{\sum_{i-1}^{n}\left(x_i - \bar{x}\right)^2}{n} \tag{5}$$

In formula (5), $\bar{x}$ is the mean of the array X_n.

For the measured axle box acceleration data $a = \{a_1, a_2, a_3, ..., a_N\}$, as shown in Figure 10, assuming the sliding window width is M, then $M < N$, and the calculation results of sliding variance are shown in Formula (6):

$$S = \{S_1, S_2, S_3, ..., S_{N=M+1}\},$$
$$S_k = \frac{\sum_{i=k}^{k+M-1}\left(a_i - \bar{a}_k\right)^2}{M} \tag{6}$$

In formula (6), there are:

$$\bar{a}_k = \frac{\sum_{i=k}^{k+M-1} a_i}{M} \tag{7}$$

According to formula (7), formula (8) can be obtained as:

$$\bar{a}_{k+1} = \bar{a}_k - \frac{a_k}{M} + \frac{a_{k+M}}{M} \tag{8}$$

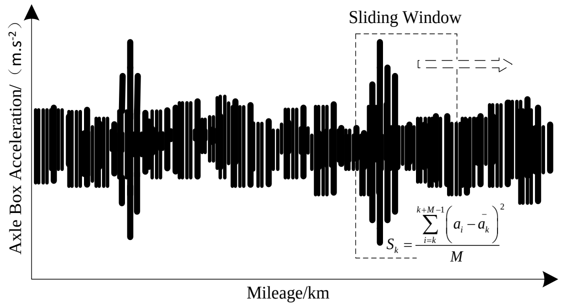

Figure10. Sliding Variance of Vertical Acceleration of Axle Box

2.2.3. Selection of Sliding Window Width

Formula (6) and formula (7) show that the key of sliding variance statistical algorithm is to determine the width of sliding window M. Two ways are considered to determine the width of sliding window M, one is to determine M (time window) based on time, as formula (9):

$$M = \frac{T}{dt} = Tf \tag{9}$$

Another method is to determine M (distance window) based on distance, as formula (10):

$$M = \frac{L}{dl} = \frac{Lf}{v} \tag{10}$$

In formula (10), L is the length of the line to be covered by the sliding window, with the unite of m; dl is the length of the line corresponding to the sampling interval, with the unite of m; f is the sampling frequency, with the unite of Hz; v is the speed of the vehicle, with the unite of m/s.

At the same speed, there is a one-to-one correspondence between the time window and the distance window [16,17]. Dynamic detection corresponds the peak value of vehicle dynamic response to the position of the line. Through the sliding variance of axle box acceleration, the line diseases and their corresponding positions can be found out. The distance window is more suitable. For the distance window, the selection of L is very important, L is too small to cover the overall response caused by a certain line excitation, and L is too large to weaken the response caused by specific line excitation. The response of typical line excitation links such as welded joints and turnouts in the speed range of 200 km/h to 350 km/h is analyzed. The response length is generally 10 m to 20 m. Therefore, it is reasonable to choose 20 m for L.

3. Results

3.1. Abnormal Vibration Detection of Shock Absorber Attenuation of Axle Box

In order to investigate the change trend of bogie's vertical vibration acceleration when the shock absorber of axle box is abnormal, the numerical simulation is carried out at first. Therefore, under the condition of insufficient hydraulic oil, it is assumed that the damping coefficient of one axle box damper in eight axle box dampers of a vehicle is 0. When the throttle hole is blocked, the damping coefficient of one of the eight axle box dampers in a vehicle is assumed to be twice as high as that of the intact axle box dampers. Based on the above assumptions, the damping coefficient of the shock absorber of axle box is calculated. Figure 11 is an example of using the method of amplitude ratio to detect the abnormality of shock absorber of axle box. Figure 12 is an example of using the method of response ratio to detect the abnormality of shock absorber of axle box.

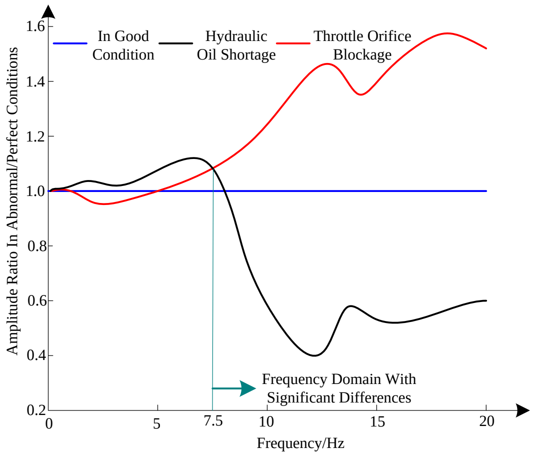

Figure 11. Detection of Shaft Box Shock Absorber Abnormality by Amplitude Ratio

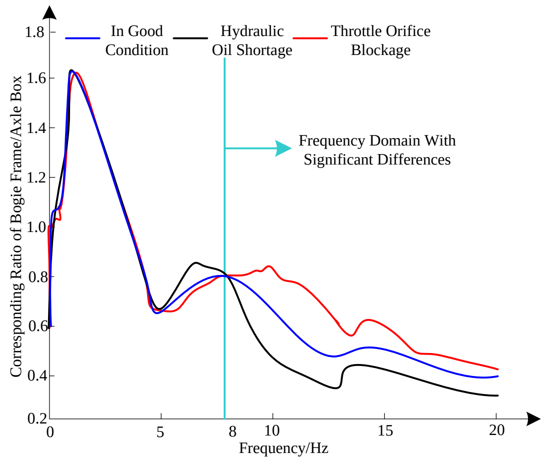

Figure 12. Detects Abnormal Vibration Attenuation of Axle Box Damper Based on Response Ratio

In Figure 11, the amplitude ratio of intact state (abnormal/intact) at each frequency is 1. From the difference of vibration attenuation characteristics of axle box dampers, in the frequency domain higher than 7.5 Hz, with the increase of vibration frequency of axle box dampers, when the throttle hole is blocked, the amplitude ratio of axle box acceleration is higher than 1, and when the hydraulic oil is insufficient, the amplitude ratio is lower than 1, which is inconsistent with the amplitude ratio of intact condition. Therefore, the shock absorber of axle box is in an abnormal state. It can be considered that the failure of the shock absorber of axle box can be judged by comparing the difference of vibration reduction characteristics in the frequency domain with the amplitude frequency domain above 7.5 Hz.

Figure 12 is an example of using response ratio method to detect the abnormality of shock absorber of axle box. From about 5 Hz, the response ratio is different, and there is also difference at 8Hz, but the difference is basically 0. After 8 Hz, the normal state, throttle hole blockage and hydraulic oil shortage show a decreasing trend with the increase of vibration frequency of the axle box's shock absorber. Although the amplitude ratio of the three is consistent, there are obvious differences. Therefore, the shock absorber of axle box is in abnormal state, and the frequency domain above 8Hz is used, which can determine the failure of shock absorber of axle box.

3.2. Line Detection by Using Sliding Variance Peak Method of Axle Box Acceleration

The main factors affecting vehicle dynamic response include vehicle type and state, vehicle speed and line disturbance. When determining the threshold value of sliding variance of axle box vertical acceleration for line detection, it should correspond to vehicle type, state and running speed. In fact, the sampling frequency of vertical acceleration of axle box also directly affects the calculation result of sliding variance. The sliding variance of the vertical acceleration of a trailer's axle box is calculated when a comprehensive inspection vehicle runs at the speed level of 300 km/h in the initial stage of a high-speed railway joint commissioning test. The sampling frequency of the axle box acceleration is 100 Hz. Statistical analysis of the length of the line is 220 km, and there is a total of about 2200 rail welded joints and 6 groups of turnouts. The peak value of sliding variance of axle box vertical acceleration corresponding to all welded joints and turnouts is calculated. Table 1 shows the peak value of sliding variance greater than the threshold value and its proportion when the threshold value is different.

Table 1. Statistical Result of Sliding Variance of Vertical Acceleration of Axle Box in 220 km Line Section

Threshold Value/(m2·s-4)	The Number of Sliding Variance Peaks Greater than the Threshold	Proportion of the Number of Sliding Variance Peaks Greater than the Threshold %
10000	0	0
8000	2	0.09
6000	5	0.22
5000	23	1.03
4000	67	2.99
3000	199	8.89
1000	1730	77.3
500	2237	99.96

The peak values of sliding variance of axle box vertical acceleration corresponding to 99% of welded joints and 6 groups of turnouts are between 500 m2/s4 and 5000 m2/s4. If 99% confidence probability corresponds, the threshold value is 5000 m2/s4. Table 2 lists the location of the line whose peak value of sliding variance of axle box vertical acceleration is more than 6000 m2/s4 and the corresponding line condition.

Table 2. Route Locations of Vertical Acceleration Sliding Variance Peak of Greater than 6000 m2/s4

Peak Value of Sliding Variance of Vertical Acceleration of Axle Box/(m2·s-4)	Corresponding Route Location	Corresponding Line Condition
8673	K823+940	Welded Joint
8468	K832+040	Welded Joint
6437	K762+520	Welded Joint
6275	K761+450	Switch
6013	K837+240	Welded Joint

The peak value of sliding variance of axle box vertical acceleration passing through all turnouts at a speed level of 300 km/h of a comprehensive testing vehicle in the initial stage of a high-speed railway joint commissioning test is made statistical analysis, in which the sampling frequency of axle box acceleration is 1000 Hz. Table 3 shows the peak value of sliding variance greater than the threshold value and its proportion when the threshold value is different.

Table 3. Statistical Results of Peak Sliding Variance of Axle Box Vertical Acceleration at Turnout

Threshold Value/(m2·s-4)	The Number of Sliding Variance Peaks Greater than the Threshold	Proportion of the Number of Sliding Variance Peaks Greater than the Threshold %
20000	0	0
15000	2	5.3
10000	3	7.9
8000	4	10.5
5000	16	42.1
4000	27	71.0
3000	31	81.6
2000	38	100

The peak value of sliding variance of axle box vertical acceleration corresponding to all turnouts ranges from 2000 m2/s4 to 20000 m2/s4, and the peak value of sliding variance of axle box vertical acceleration greater than 8000 m2/s4 has only 4 turnouts, accounting for about 10% of all turnouts. If 90% confidence probability corresponds, the threshold value is 8000 m2/s4.

Rail pre-grinding can eliminate decarburization layer on rail surface, short wave irregularity during rolling and rail surface defects during construction, and improve the smoothness of rail welded joints. Figure 13 shows the sliding variance of vertical acceleration of axle box at the speed level of 300 km/h before and after rail pre-grinding in 10 km section of a high-speed railway.

Figure 13 shows that the effect of rail pre-grinding on improving the smoothness of rail welded joints is very obvious. After rail pre-grinding, the transient vibration energy of wheel pairs at rail welded joints generally decreases by 5-10 times.

3.3. Derailment Detection

3.3.1. Basic Ideas

In previous research work, a method of comparing the frequency of acceleration exceeding the critical value and the cumulative value of current and previous acceleration is proposed. In order to improve the detection accuracy of derailment, this paper focuses on the different phenomena of peak vibration acceleration at specific parts of the vehicle and the positive and negative asymmetry of the inherent vibration acceleration when derailment occurs. The peak vibration acceleration here refers to the maximum vibration acceleration in a certain period of time. This method considers that "if the running speed and track state are determined, the magnitude of positive/negative peak vibration acceleration of bogie frame and vehicle body can be roughly determined". According to the combination of running speed level (e.g. step length 10 km/h) and each track state (classification) (e.g. line interval level), the statistical average value and standard deviation value of peak vibration acceleration are established in advance. In the database, by comparing the database data with the peak vibration acceleration of the running time in turn, the abnormality of the running device can be detected. In addition, according to the positive and negative asymmetry of vibration acceleration waveform and other factors, it is determined whether derailment will occur. The following is the confirmation of the sample distribution (the distribution of vibration acceleration in normal condition) which belongs to the first stage of the same-level method, and the method for quantifying the degree of deviation of vibration acceleration from normal condition when derailed by checking the distribution of vibration acceleration in normal condition.

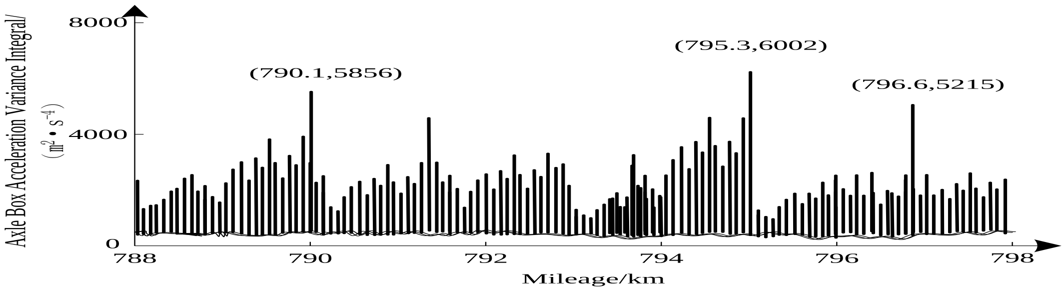

(a) Before Grinding

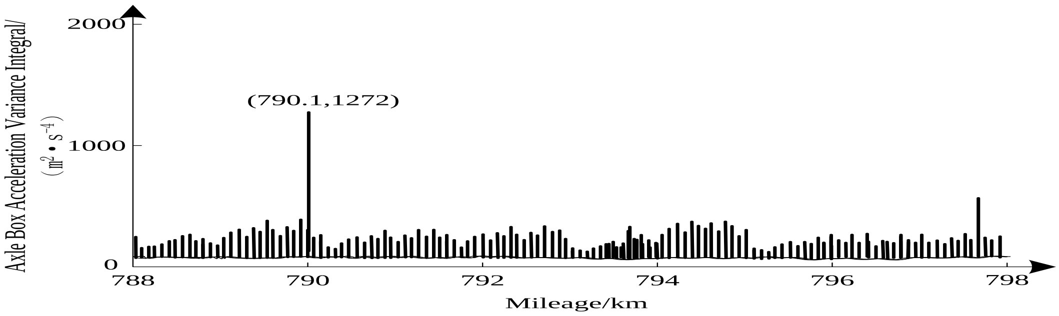

(b) After Grinding

Figure 13. Sliding Variance of Vertical Acceleration of Axle Box before and after Rail Grinding in the Same Line Section

3.3.2. Research on Detection Method

(1) Normal operation

Firstly, the statistical distribution of peak vibration acceleration in normal operation is confirmed. Figure 14 is the vertical vibration acceleration waveform of the freight vehicle body with a 2-axle bogie in normal operation. Figure 15 and Figure 16 show the peak vibration acceleration of the waveform calculated at regular intervals, respectively, and the statistical results of peak vibration acceleration are expressed in terms of frequency distribution. Table 4 gives the mean and standard deviation of normal operation.

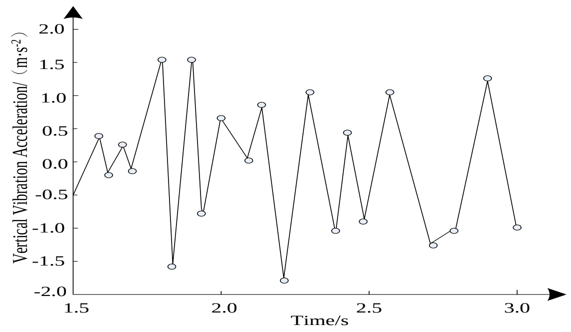

Figure 14. Vertical Vibration Acceleration Waveform of Vehicle Body in Normal Operation

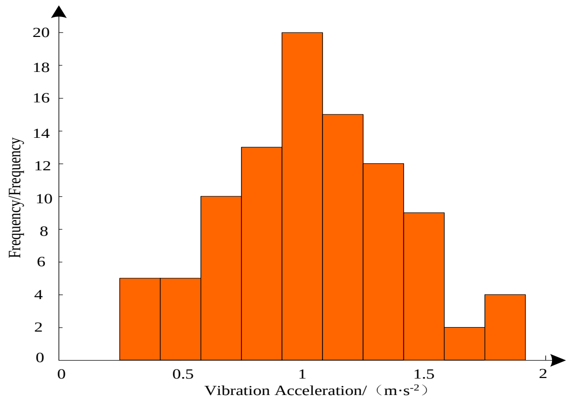

Figure 15. Frequency Distribution of Positive Peak Vibration Acceleration

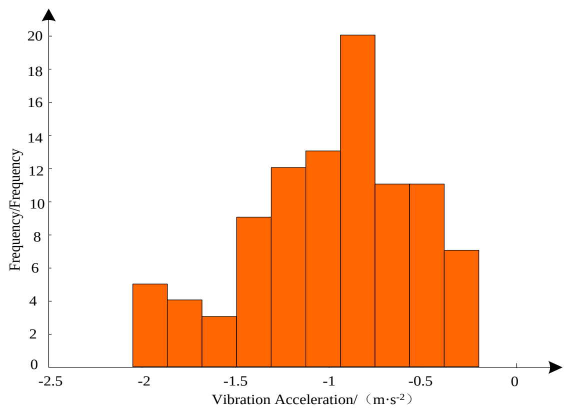

Figure 16. Frequency Distribution of Negative Peak Vibration Acceleration

Table 4. Average and Standard Deviation of Vertical Vibration Acceleration of Vehicle Body under Normal Operation

	Average Value	Standard Deviation
Positive Peak Vibration Acceleration/(m·s-2)	1.07	0.36
Negative Peak Vibration Acceleration/(m·s-2)	-1.00	0.43

The number of sampling samples is about 100, which is not enough, but the peak vibration acceleration shown in Figure 15 shows a normal distribution. From the negative peak vibration acceleration shown in Figure 16, the distribution shape is approximately lognormal distribution and F distribution. The higher the frequency around the average is, the more it deviates from the average, and the lower the frequency distribution is. According to these conditions, the more the deviations from the average are, the greater the possibility of anomalies is.

Table 4 gives the mean and standard deviation of normal operation. In addition, the vehicle speed corresponding to the test data of derailment is 9 km/h, so the comparison with the vertical vibration acceleration of the vehicle body under normal operation at this speed is in line with the requirements. However, because the data of freight vehicle running at 9 km/h in derailment test cannot be obtained, as the data of normal operation, the same data of freight vehicle running at 60 km/h with 2-axle bogie are used. The vibration acceleration of vehicle body increases with the increase of speed, so the derailment detection described below is conservative, and it is considered that there is no problem to compare with the vibration acceleration of 60 km/h running speed.

(2) Derailment operation

Figure 17 shows the vertical acceleration waveform of the vehicle body when the truck derails. In this paper, the acceleration is in the downward direction, and the acceleration waveform is processed in the same way as in normal operation. The peak vibration acceleration (Formula (11), (12)) is compared with the standard deviation in normal operation.

$$\alpha p > 30\sigma p \quad (11)$$

$$\alpha n < -50\sigma n \quad (12)$$

In the formula, σp is the standard deviation of positive peak vibration acceleration in normal operation, with the unit of m/s2; σn is the standard deviation of negative peak vibration acceleration in normal operation, with the unit of m/s2; αp is the positive peak vibration acceleration when derailing, with the unit of m/s2; αn is negative peak vibration acceleration when derailing, with the unit of m/s2. In addition, Figure 17 is the vibration acceleration of the vehicle body when derailing, and Figure 18 is the vibration acceleration of the replaced bogie when running on ballast track.

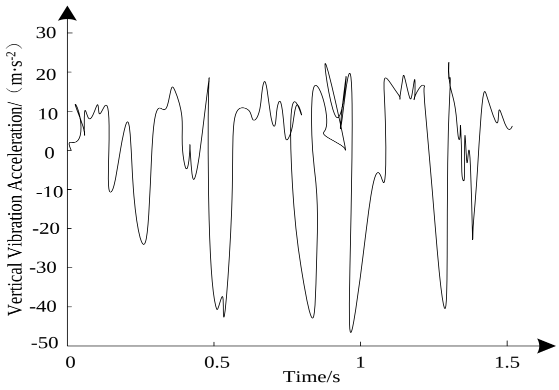

Figure 17. Vibration Acceleration of Car Body When Derailing

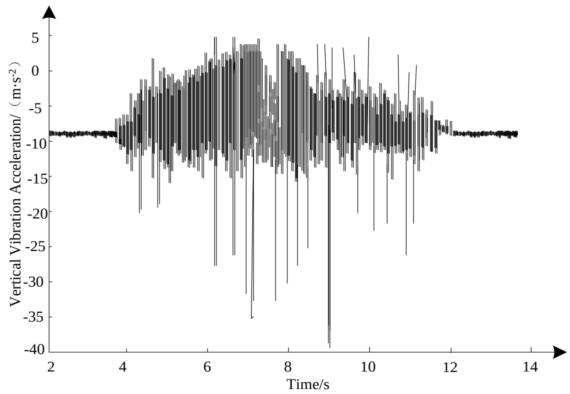

Figure 18. Vibration Acceleration of Replaced Bogie Running on Ballast Track

From Fig. 14 and 17, it can be seen that the vertical vibration acceleration of axle box fluctuates between -1.8 m·s-2 and 1.7 m·s-2 in normal operation, with a small fluctuation range. When the vehicle derails, the vertical vibration acceleration of axle box fluctuates irregularly between -45 m·s-2 and 22 m·s-2. The fluctuation range is very large, and the absolute value of negative peak vibration acceleration is greater than that of positive peak vibration acceleration. When derailment occurs, the vertical vibration acceleration of axle box is abnormal. After installing acceleration sensor on the bogie after replacement, it runs on ballast track. Figure 18 is the vibration acceleration of the replaced bogie running on ballast track. The vertical vibration acceleration shown in Figure 18 is the same as that shown in Figure 17. When the vehicle derails, the absolute value of the negative peak vibration acceleration is greater than the positive peak vibration acceleration, and the vertical vibration acceleration of the axle box is abnormal. In Figure 18, the reason for the formation of vibration acceleration waveform is that ballast and sleepers cause the wheel to be impacted in the upward direction, which is the waveform with unique characteristics when the vehicle derails. In addition, the sleepers are usually laid at intervals of 34 to 44 per 25 m. Assuming that the running speed is 9km/h when derailment is considered, it can be considered that the wheel of the test vehicle passes through a sleeper at intervals of 0.30 s to 0.23 s. In Figure 17, the time interval of negative peak vibration acceleration is about 0.25 s, which is consistent with the time when the wheel passes through the sleeper. Therefore, it can be considered that the impact of sleepers and wheels results in negative peak vibration acceleration of the vehicle body. It can be seen that the accuracy of derailment detection can be improved by considering the time when the wheel passes through the sleeper. In addition, even on slab (ballastless) track, the accuracy of derailment detection can be improved if the track information is used as the basis.

4. Conclusions

This paper studies the detection method for acceleration sensor anomaly of axle box of unmanned vehicle. This method takes the failure of bogie parts directly related to operation safety and the sliding variance peak value of dynamic response index of railway vehicle as the influencing factors to judge the acceleration sensor anomaly detection of axle box of unmanned vehicle, to achieve the acceleration sensor anomaly detection of axle box of unmanned vehicle.

(1) From the difference of vibration attenuation characteristics of axle box dampers, in the frequency domain above 7.5 Hz, the amplitude ratio of axle box acceleration under the condition of throttle hole blockage and insufficient hydraulic oil is inconsistent with that under the intact condition, which indicates that the axle box damper is abnormal at this time. Therefore, the difference of vibration attenuation characteristics in this frequency domain can be determined by comparing the amplitude frequency domain above 7.5 Hz. When the response ratio method is used to detect the shock absorber abnormality of the axle box, the frequency domain of the response ratio difference is more than 8 Hz. When the response ratio of the axle box acceleration is higher than 8 Hz, the response ratio of the axle box acceleration under the three conditions is consistent, but there are obvious differences, which indicate the shock absorber abnormality of the axle box. Therefore, the failure of shock absorber of axle box can be judged by using the difference of response rate in frequency domain above 8 Hz. Therefore, comparing the difference of vibration attenuation characteristics of axle box damper and using the method of response ratio to detect the abnormality of axle box damper, can well judge the abnormal condition of axle box acceleration, so as to realize the abnormal detection of axle box sensor acceleration of unmanned vehicle.

(2) Rail pre-grinding has obvious effect on improving the smoothness of rail welded joints. Based on the sliding variance of vertical acceleration of axle box at 300 km/h speed level, the instantaneous vibration energy of wheelset at rail welded joints after rail pre-grinding generally decreases by 5-10 times, and the variance of axle box acceleration significantly decreases. The variance of axle box acceleration reflects the vibration energy of wheelset. It can effectively characterize the influence of line excitation on the vibration state of wheelset.

(3) When derailment occurs, the vertical vibration acceleration waveform of axle box and the vibration acceleration waveform of replaced bogie running on ballast track are both the absolute value of negative peak vibration acceleration greater than that of positive peak vibration acceleration, and the vertical vibration acceleration of axle box is abnormal.

Reference

[1] Sun, Q.; Zhang, B.; Li, Y.P.; Chen, C.J. Wavelength-Fixing Mechanisms for Detecting the Wheel Polygon-Shaped Fault Onsite. Journal of Railway Science and Engineering,15, 2018,2343-2348.

[2] Wang, S.F.; Zhang, D.W. Analysis of Limit Relationship between Vehicle Speed and Front Wheel Angle. Machinery Design & Manufacture, 9,2017 , 237-240.

[3] Xu, N.; Ren, Z.S.; Xu, R. Time and Frequency Domain Response and Vibration Transfer Characteristics of High-Speed EMU. Journal of the China Railway Society, 41, 2019, 31-40.

[4] SHI Chunfei;SUN Yi;WANG Xiaoping. Study on Highly Sensitive Detection of Polarization ControlledLight Intensity Modulated SPRi Sensor[J]Chinese Journal of Sensors and Actuators. 30,2017,1152-1157. [5]LIU Yong-yong LI Guo-ping ZUO Guo-kun.Design of force sensor signal acquisition and processing system based on STM32[J].Transducer and Microsystem Technologies. 36,2017,112-115.

[6] Dong, W.; Huang, W.; Xing, Z.Y.; Long, J.; A Rail Corrugation Detection Method Based on Wavelet Packet-Energy Entropy. Railway Standard Design, 62, 2018, 52-58.

[7] Li, C.B.; Lou, J.J.; Zhang, Z.H.; Xia, J.M. Experimental Study on Vibration Characteristics of a Star-Type Compressor. Journal of Wuhan University of Technology (Transportation Science & Engineering),42, 2018, 23-28.

[8] Yang, Y.; Ding, J.J.; Li, F.; Jiang, K. Effect of Equivalent Stiffness of Resilient Wheel on Vehicle Dynamic Performance. China Railway Science,39, 2018,65-72.

[9] Huang, Y.S.; Deng, S.E.; Zhang, W.H.; Hu, J.; Sun, L.M.; Ma, Z.K. Influence of Impact Loads on the Dynamic Characteristics of Plastic Cages in Railway Axle Bearings. Journal of Vibration and Shock, 37, 2018,172-180.

[10] Cha, H.; Ren, Z.S.; Xu, N. Vibration Performance of High-Speed Vehicles with Axle Box Bearing. Journal of Mechanical Engineering,54, 2018,144-151.

[11] Wang, W.J.; Li, G.Q.; Han, J.C.; Li, Q.Z. Influence Rule of Dynamic Stress of High-Speed Train Gearbox Housing. Journal of Traffic and Transportation Engineering, 15,2019, 85-95.

[12] Dai, M.Z.; Gao, C.F. Framework Performance Evaluation Based on Hadoop, Spark and Flink Large-Scale Data Analysis. Journal of China Academy of Electronics and Information Technology, 13,2018, 149-155.

[13] Guo, Q.Y.; Kang, J.S.; Feng, J.H.; Zhou, G.F. Current Development and Trend of Rail Transit Vehicle Traction Control. Journal of Power Supply, 15, 2017, 40-45.

[14] An, Y.P.; Zhao, J.C.; Liu, J.N. Research on Control of Lithium-Ion Battery Charge and Discharge Based on Bi-Directional DC/DC Converter. Chinese Journal of Power Sources,41, 2017,208-210.

[15] Yu, F.H. Design and Analysis of Intelligent Three Dimensional Parking Lot Control System Based on PLC Technology. Automation & Instrumentation, 231, 2019, 86-88.

[16] Wang, D.X.; Teng, J.K. Authentication Scheme Based on Aggregate Signature in VSNs. Journal of Jilin University (Science Edition), 56, 2018, 657-662.

[17] Liu, B.; Luo, X.; Zhu, J. Research on Simulation of Planning Obstacle Avoidance Path for Automated Vehicles. Computer Simulation, 35, 2018, 105-110.